Acta metall. Vol. 33, No. 7, pp. 1339–1354, 1985
Printed in Great Britain

0001-6160/85 $3.00 + 0.00
Pergamon Press Ltd

FATIGUE CRACK GROWTH DUE TO PERIODIC UNDERLOADS AND OVERLOADS

N. A. FLECK
Cambridge University Engineering Department, Trumpington Street, Cambridge CB2 1PZ, England

(*Received* 11 *April* 1984; *in revised form* 18 *July* 1984)

Abstract—Fatigue cracks in steels and aluminium alloys can grow at a faster rate than predicted by a linear summation of damage, when they are subjected to certain types of load history. A number of mechanisms, including crack closure, can be invoked to explain this acceleration effect. An investigation into the influence of periodic underloads and overloads on crack growth response was conducted for BS4360 50B structural steel, BS1501 32A pressure vessel steel and 2014A-T4 aluminium alloy. A computer-controlled load shedding technique enabled tests to be run under stress intensity, K, control. It was found that cracks in all three materials grow at nearly twice the rate predicted by a Miner-type linear summation of damage. Measurements showed that crack closure does not account for these small changes in crack growth rate. A combination of other mechanisms leads to the accelerated growth.

Résumé—Des fissures de fatigue peuvent croître dans des aciers et des alliages d'aluminium, avec une plus grande vitesse que celle qui correspond á une sommation linéaire du dommage, lorsqu'on les soumet à certains types d'histoire de charge. On peut invoquer un certain nombre de phénomènes, y compris une fermeture des fissures, pour expliquer cette accélération. Nous avons étudié l'influence de souscharge et de surcharges périodiques sur la croissance des fissures dans un acier structural BS 4360 50B,dans un acier BS1501 32A pour conteneur à haute pression et dans un alliage d'aluminium 2014A-T4. Une technique de délestage contrôlé par ordinateur a permis d'effectuer des essais en contrôlant le facteur d'intensité de la contrainte K. Dans ces trois matériaux, nous avons trouvé que les fissures croissaient avec une vitesse pratiquement double de celle que prévoit une sommation linéaire du dommage de type Miner. Des mesures ont montré que la fermeture des fissures ne rendait pas compte de ces petites variations de la vitesse de croissance des fissures. C'est une combinaison d'autres mécanismes qui conduit à la croissance accélérée.

Zusammenfassung—Ermüdungsrisse können sich in Stählen und Aluminiumlegierungen viel rascher, als aus einer linearen Summierung der Verformungsschädigung folgen würde, ausbreiten, wenn sie einer gewissen Verformungsgeschichte unterworfen werden. Dieser Beschleunigungseffekt kann mit einer Vielzahl von Mechanismen erklärt werden, darunter die Rißschließung. Der Einfluß Periodischer Unter- und überlastung auf das Rißwachstum wurde an dem strukturierten Stahl BS4360 50B, dem Kesselstahl BS 1501 32A und der Aluminiumlegierung 2014A-T4 untersucht. Rechnerkontrolle erlaubte, die Versuche unter Steuerung der Spannungsintensität durchzuführen. Nach diesen Versuchen wachsen Risse in allen drei Werkstoffen fast zweimal so schnell wie von von einer Miner-ähnlichen Summierung der Verformungsschädigung vorausgesagt. Messungen zeigen, daß R-ßschließung diese geringen Veränderungen in der Rißwachstumsrate nicht erklären kann; eine Kombination der anderen Mechanismen verursacht das beschleunigte Wachstum.

INTRODUCTION

When a fatigue crack is subjected to variable amplitude loading it may grow at a faster or slower rate than predicted by a linear summation of damage. Here, linear summation of damage is the crack growth due to constant amplitude loading of magnitude equal to the variable amplitude load history. A well-known example of retarded growth is the case of a single peak overload: when a long fatigue crack is subjected to constant amplitude loading followed by a single peak overload, the crack slows down by several orders of magnitude [1–3]. In contrast, periodic underloads and overloads induce slight changes in growth rate [4, 5]. The phenomenology and modelling of these subtle load interaction phenomena form the subject of this paper.

Periodic underloads are similar to the actual service load histories experienced by a number of engineering components:

(1) Gas storage vessels can be subjected to a daily cycle which consists of loading to a constant maximum pressure and discharging to various pressures depending on the demand [6].

(2) Gas turbine blades experience constant amplitude high frequency stress cycles due to vibrations; superimposed on these small cycles is a much larger run-down/start-up load cycle [7].

(3) Railway lines suffer random loading at constant maximum stress, each time a train passes [8].

(4) Aircraft wings experience gust loading at high mean stress during flight, and a large underload each time the aeroplane lands and takes off again [9].

Similarly, periodic overloads are experienced by a large number of engineering components. For example, each time power generation equipment, such as a turbo-generator, starts-up an overload is applied to the rotor and bearings. Operator misuse and occasional, extreme operating conditions are further common sources of periodic overloads.

In this study, accelerated growth due to variable amplitude loading is reviewed. The crack growth responses of two low strength steels and a medium strength aluminium alloy are determined, for the case of periodic underloads and periodic overloads. The magnitude of loading is chosen such that growth rates are in the mid-regime of the Paris plot: growth rates are far above threshold. Finally, the mechanisms which cause the periodic underloads and periodic overloads to display accelerated and retarded growth are critically evaluated in the light of these tests results.

PREVIOUS WORK

A search through the literature reveals that certain types of load history lead to accelerated growth. The mechanism causing faster growth may differ in each case.

1. *Programmed and random loading with constant* K_{max}

Broek and Leis [10] have tested centre-cracked sheets made from 7075-T6 aluminium alloy, using the load histories of Fig. 1(a). Cracks grew 60% faster than predicted by linear summation. Broek and Leis suggested that the large amplitude cycles of each load block damaged or pre-strained material at the crack tip, such that accelerated growth accompanied the smaller cycles.

McMillan and Pelloux [11] applied the programmed load histories shown in Fig. 1(b) to centre-cracked specimens made from 2024-T3 aluminium alloy. For a crack growth increment of less than 0.08 mm per load block, they found an acceleration factor, γ, of 2, where

$$\gamma = \frac{\text{measured growth rate per block}}{\text{predicted growth rate per block by a linear summation of the constant amplitude crack growth response}}. \quad (1)$$

At faster growth rates, the test-pieces underwent net section yield and crack growth retardation occurred.

2. *Step increase in mean stress*

It is well known that a step increase in mean stress causes an accelerated fatigue crack growth transient [12, 13]. Hertzberg [14] argues that the high growth rates at the beginning of the high block in low-high block loading are due to crack closure. During the first few cycles of the high load block, the crack opening load gradually increases from that associated with the low load block to that associated with the high load block. Consequently, the portion of the stress intensity range for which the crack is open, ΔK_{eff}, is larger than the constant amplitude value, and accelerated growth results. Trebules *et al.* [13], using 2024-T3 aluminium alloy subjected to this type of loading, have observed transient fatigue crack growth at more than three times the rate associated with constant amplitude loading.

The first cycle of high load application in a low-high block loading test, repeated overloads or single peak overload test produces an anomalously large crack growth increment, known as a giant striation [11, 15, 16]. The giant striation may be an order of magnitude larger than the striation spacing for an equivalent constant amplitude load cycle. Such accelerations have been found for steels, and aluminium, titanium and copper alloys [16]. The phenomenon has been successfully described using a crack closure approach, and also an elastic–plastic crack opening displacement model [16].

3. *Two- or three-step loading near threshold*

Conventionally, a single peak overload or multiple peak overloads retard subsequent crack growth due to a combination of residual stress and closure effects [14].

Koterazawa [15] has shown that block loading consisting of two cycles of fully reversed overstress followed by 10^4–10^7 cycles of understress can give rise to an acceleration factor, γ, of more than 100, see Fig. 2(a). Faster growth was noted for low, medium and high strength steels and for the aluminium alloy 5052-0. Crack propagation accompanied both the understress cycles (below ΔK_{th}) and the overstress cycles (above ΔK_{th}). Closure measurements were unable to explain the accelerated growth; instead, the acceleration effect was ascribed to a zig-zag crack propagation mechanism, in conjunction with a radial dislocation structure at the crack tip due to the periodic overstressing.

In contrast to the findings of Koterazawa [15], Nisitani and Takao [17] and Kikukawa *et al.* [18] used crack closure observations to explain load interaction effects near threshold. Nisitani and Takao conducted rotating bend tests on annealed 0.54% carbon steel and quenched-and-tempered 0.54% carbon steel. Two-step loading tests of low-high-low type, Fig. 2(b), were employed. For the annealed material, they found that the high load block depressed K_{op} to below the crack opening level characteristic of the low load blocks. Accelerated growth then accompained the second low load block. A much smaller but similar effect was noted for the hardened steel.

Kikukawa *et al.* [18] observed accelerated growth in 0.38% carbon steel and A5083-0 aluminium alloy, when subjected to two- and three-step loading near threshold, Fig. 2(c). The load ratio, R, (= minimum load/maximum load of fatigue cycles) was held at 0. Crack propagation accompanied sub-threshold load-

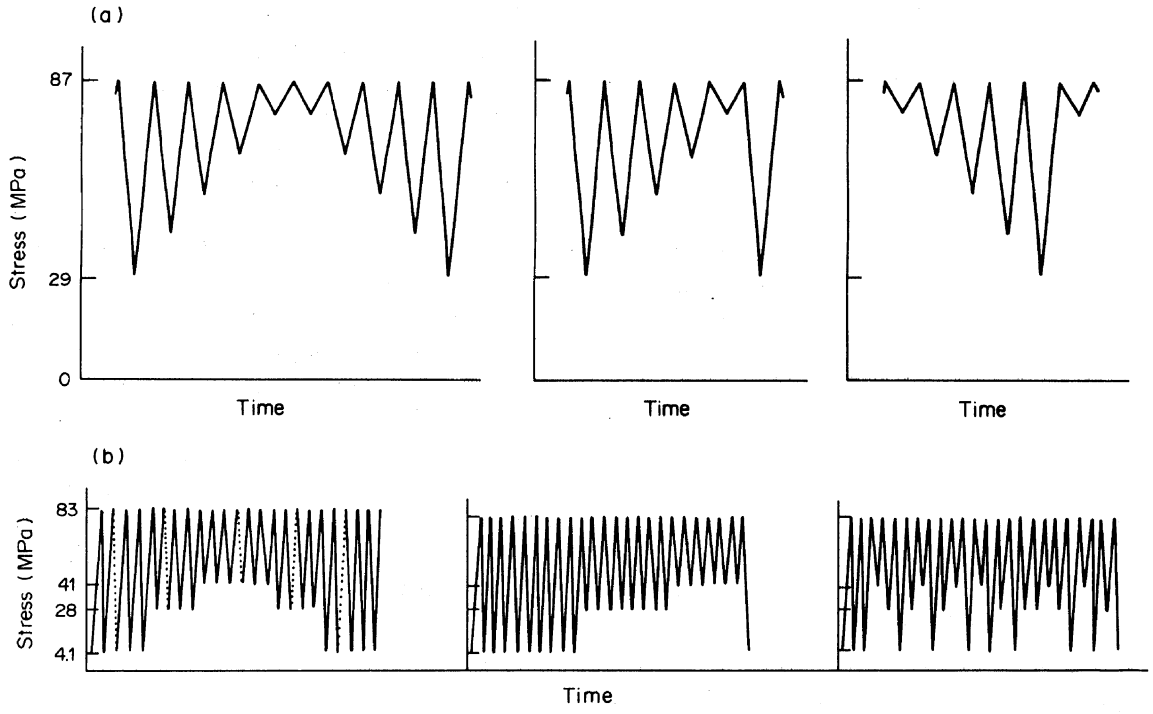

Fig. 1. Load histories with constant maximum load, known to produce accelerated growth. (a) 7075-T6 aluminium alloy. Acceleration factor, $\gamma \approx 1.6$. From Ref. [10]. (b) 2024-T3 aluminium alloy. Acceleration factor, $\gamma \approx 2$. From Ref. [11].

$$\text{Acceleration factor, } \gamma = \frac{\text{measured crack growth rate per block}}{\text{predicted growth rate per block by a linear summation of the constant amplitude crack growth response}}.$$

ing, in agreement with the findings of Koterazawa [15]. The acceleration phenomenon was explained in terms of crack closure, by noting that the constant amplitude threshold effective stress intensity range, $(\Delta K_{eff})_{th}$, was reduced by the variable amplitude loading. Kikukawa *et al.* were thus able to account for increases in crack growth rate by more than two orders of magnitude.

Crack closure arguments have also been used to account for retarded near threshold growth. Suresh and Ritchie [19] reported that an injection of 2.7×10^6 load cycles below ΔK_{th} retarded the crack

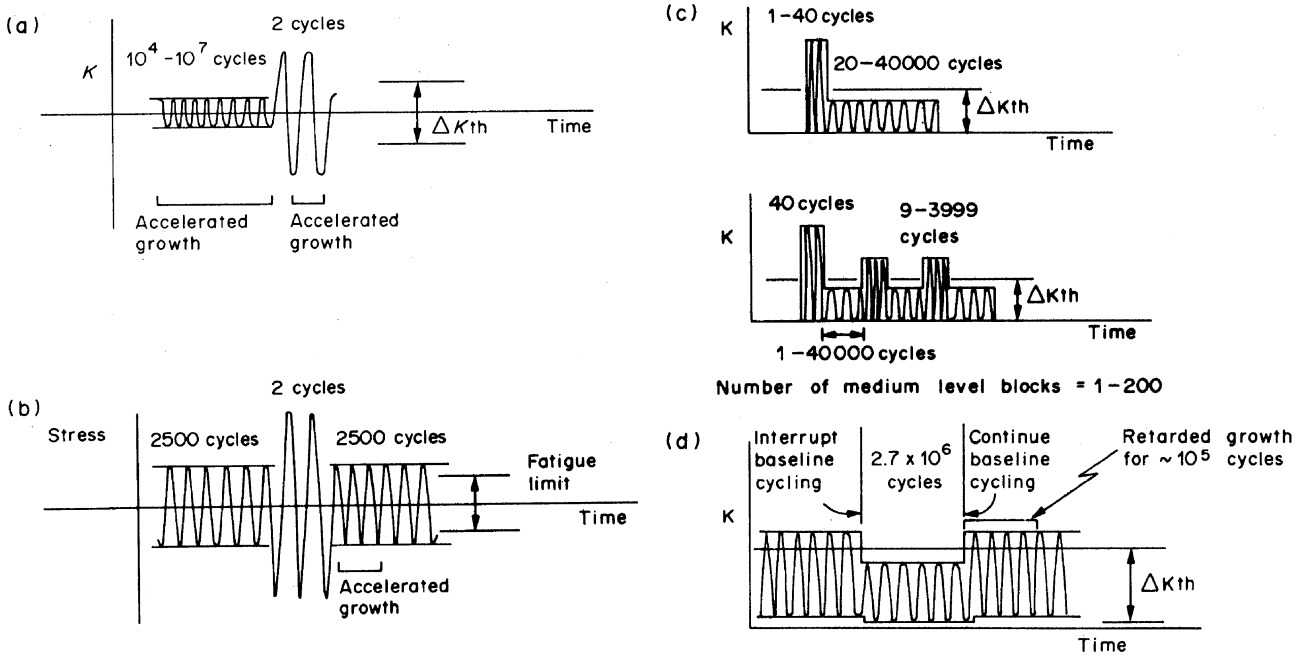

Fig. 2. Two and three level block loading near threshold, known to give accelerated growth. (a) Low, medium and high strength steels, and 5052-0 aluminium alloy. From Ref. [15]. (b) Annealed 0.54% carbon steel, and quenched-and-tempered 0.54% carbon steel. From Ref. [17]. (c) Normalised 0.38% carbon steel and A5083-0 aluminium alloy. From Ref. [18]. (d) A542 class 3 pressure vessel steel. From reference [19].

growth associated with subsequent baseline cycling at just above ΔK_{th}, Fig. 2(d). No growth accompanied the small cycles. They employed compact tension specimens made from A542 class 3 pressure vessel steel, and used a load ratio, R, of 0.05 for each load history. They argued that the small cycles increased the fretting damage and oxide thickness on the fracture surfaces near the crack tip. Oxide-induced crack closure thereby increased and caused a retardation in crack growth rates, on re-application of the larger cycles at loads above ΔK_{th}. Unfortunately, no closure measurements were taken to substantiate their hypothesis.

4. *Other types of load history*

We might expect periodic overloads to give retarded growth since they resemble a single peak overload and repeated overloads. Such is not always the case.

Broek and Leis [10] employed load histories of the type shown in Fig. 3. They observed that fatigue cracks in 7075-T6 aluminium alloy grew up to 60% faster than predicted by linear summation. They postulated that the large cycles damaged material at the crack tip so that accelerated growth accompanied the smaller cycles.

More recently, Gurney [20] has examined the acceleration effect exhibited by BS4360 50B steel fillet welded joints when subjected to the load histories shown in Fig. 4. The specimens consisted of a 12.5 mm thick plate, with a longitudinal attachment welded centrally on each surface. A comparison of actual lives with those predicted using linear summation is included in Fig. 4. Gurney measured an acceleration factor, γ, of up to 1.7. When the ratio, ϕ, of small cycle amplitude to large cycle amplitude was varied, it was found that maximum acceleration occurred for $\phi = 0.5$, see Fig. 5. No physical basis for these results was put forward.

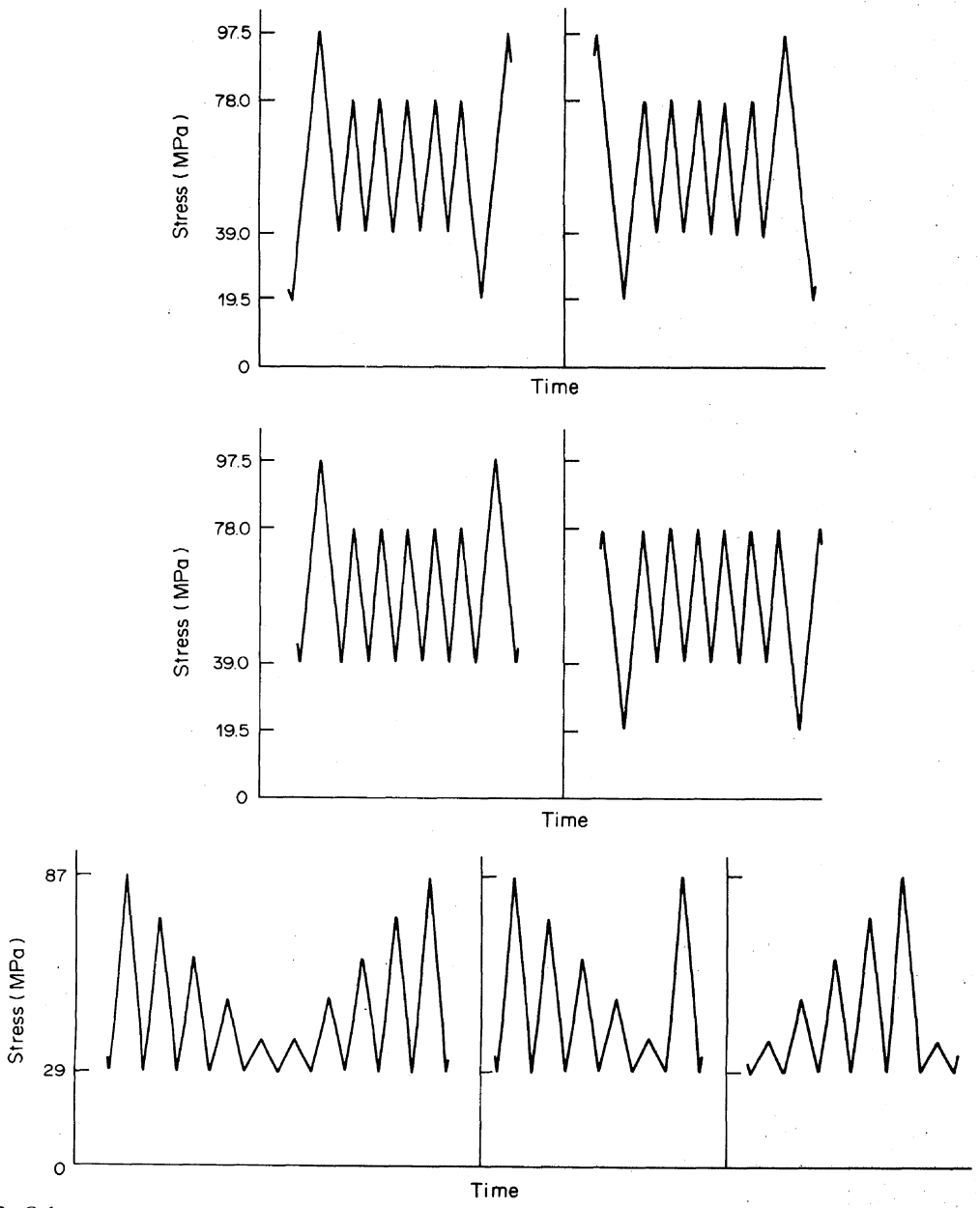

Fig. 3. Other types of load history which produce accelerated growth. Test details: 7075-T6 aluminium alloy. Acceleration factor, γ, = 1–1.6. From Ref. [10].

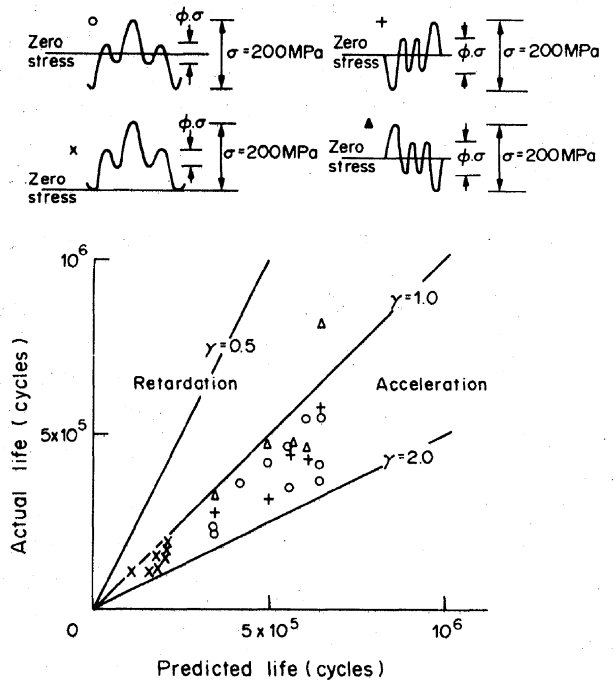

Fig. 4. Accelerated growth found by Gurney [20], for stress-relieved fillet welded joints made from BS4360 50B steel. ϕ lies in the range 0–1.

The problem of scatter

Unfortunately, most of the tests described in the preceding sections were conducted under load control, such that the stress intensity range, ΔK, and crack growth rate, da/dN, increased with crack length. The scatter in growth rate and life for these tests was often greater than a factor of 2, making any small acceleration effect difficult to quantify. Gurney [20] has published stress-life curves for the BS4360 50B material subjected to constant amplitude loading. The scatter in life was of the same order of magnitude as the acceleration effect he was investigating, as can be seen from Fig. 5.

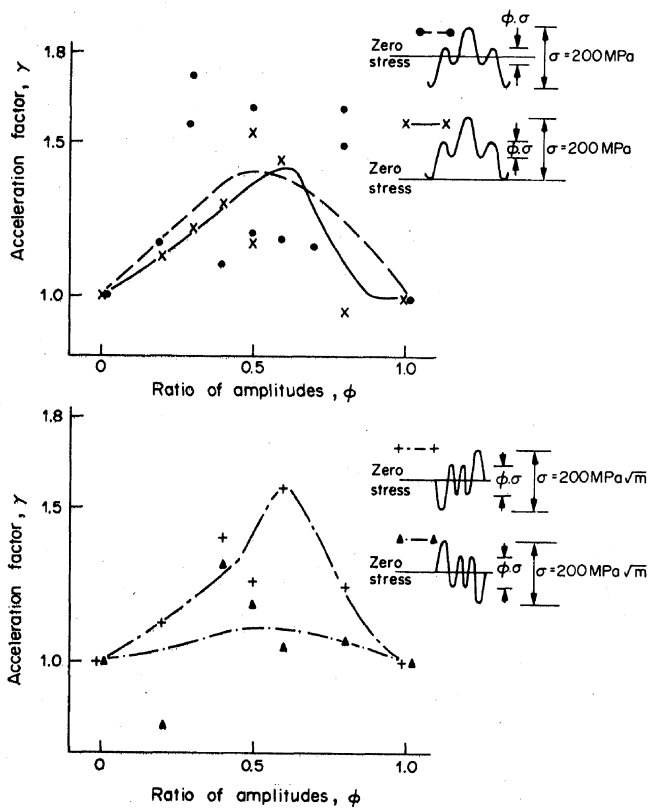

Fig. 5. Accelerated growth in stress-relieved fillet welded joints made from BS4360 50B steel. Data taken from Ref. [20].

In the present study, tests were performed using stress intensity, K, control: the applied load was shed as the crack length increased such that the stress intensity history and crack growth rate were held constant. Preliminary tests showed that the scatter in measured growth rate was then $\pm 5\%$, for specimens from the same batch of material.

EXPERIMENTAL

Tests were performed on two low strength ferritic-pearlitic steels, namely BS4360 50B structural steel and BS1501 32A pressure vessel steel. A few tests were also conducted on the single phase aluminium alloy 2014A-T4; this alloy is closely related to those used in aircraft wing manufacture. Hence, the materials chosen for this study experience periodic overloads and underloads in service.

Compact tension (CT) specimens of thickness 3 and 24 mm were cut from a single sheet of BS4360 50B steel plate. CT specimens were also cut from a 24 mm thick BS1501 32A steel plate and from a 6 mm thick 2014A-T4 aluminium alloy plate. All test-pieces were 50 mm wide and machined such that cracks grew transverse to the rolling direction. The steel specimens were stress-relieved for 1 h at 650°C prior to testing, while the aluminium specimens were tested in the as-received condition. Compositions, grain sizes and tensile properties of the three materials are given in Table 1.

Fatigue tests were performed under stress intensity control, using the waveforms shown in Fig. 6. First, the number of minor cycles, n, between major cycles was varied from 1 to 1000, with the ratio, ϕ, of amplitude minor cycle/major cycle held at 0.5. Second, the ratio ϕ was varied from 0 to 1, with the number of minor cycles per major cycle, n, held at 10. The stress intensity factor range for the major cycles, ΔK_{major}, was 25 MPa$\sqrt{m}$ for the steel specimens and 8 MPa$\sqrt{m}$ for the aluminium alloy specimens, corresponding to a constant amplitude crack growth rate of 10^{-4} mm/cycle in each case. The load ratio, R, (= minimum load/maximum load) for major cycles was held constant at 0.5. The frequency of the major cycles was 5 Hz, while the frequency of the minor cycles was $5/\phi$ Hz.

An Apple II microcomputer was used to both control each test and monitor crack length and cycles. Development of the computer control system is given in Ref. [21]. The microcomputer shed the applied load at crack growth increments of 0.1 mm in order to maintain K control to within 1%. Crack growth from the starter notch of 15 mm to a final crack

Table 1. Composition and tensile properties of test materials

Material	Composition (%)	Average grain size (μm)
BS4360 50B structural steel	0.14 C 1.27 Mn 0.41 Si 0.017 P 0.004 S 0.073 Al, Remainder Fe.	10
BS1501 32A pressure vessel steel	0.16 C 1.06 Mn 0.26 Si 0.020 P 0.003 S 0.10 Cr 0.05 Mo 0.14 Ni, Remainder Fe.	12
2014A-T4 aluminium alloy	4.4 Cu 0.50 Mg 0.80 Mn 0.70 Si, Remainder Al	60

	Tensile properties normal to rolling direction			
Material	Yield stress (MPa)	Ultimate tensile stress (MPa)	Elongation on a gauge length of 25.4 mm (%)	Strain hardening index
BS4360 50B structural steel	352	519	36	0.27
BS1501 32A pressure vessel steel	388	542	40	0.25
2014A-T4 aluminium alloy	325	446	25	0.17

length of 30 mm was monitored using the d.c. potential drop method.

Crack closure measurements were taken at 0.05 Hz using a crack mouth gauge, near tip clip gauge and a back face strain gauge. Increased sensitivity was achieved through use of an offset circuit [22].

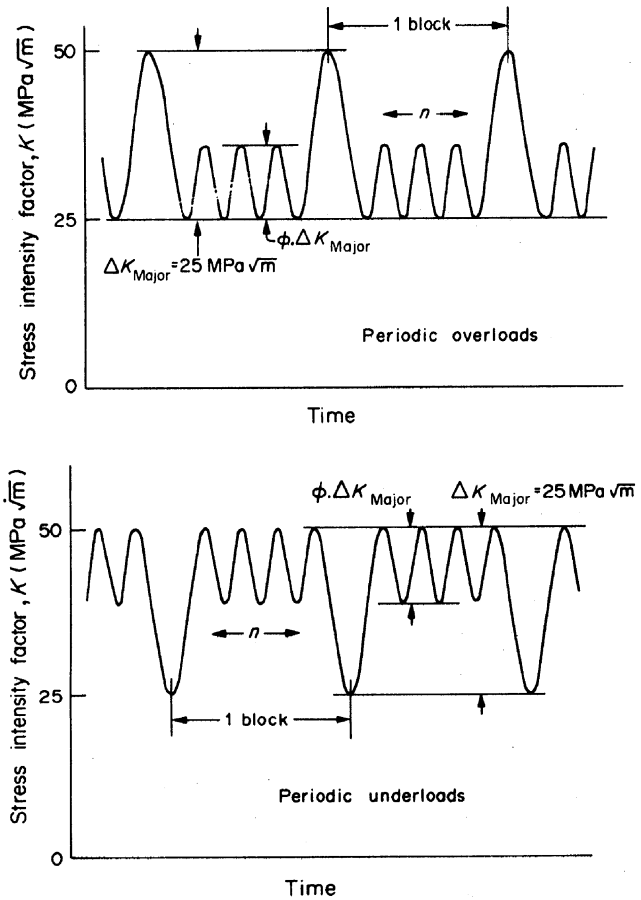

Fig. 6. Definition of load histories used in present study.

CRACK GROWTH RESPONSE

A plot of crack length, a, against number of fatigue cycles, N, for a typical test is given in Fig. 7. Initially, the crack grew slowly from the notch root of nominal radius 0.1 mm; thereafter the crack growth rate was constant.

Periodic underloads

The effect of varying the number, n, and amplitude, ϕ, of minor cycles upon fatigue crack growth is shown in Table 2 and Figs 8 and 9. Accelerated growth was observed for all values of n and ϕ. The limited data shows that γ is little influenced by test material, or by a change in stress state from plane stress (3 mm thick BS4360 50B specimens) to plane strain (24 mm thick BS4360 50B specimens). The acceleration factor, γ, reaches a maximum of 1.5–1.8, for $n = 10$ and $\phi = 0.5$, see Figs 8 and 9. As n increases to a large value of 1000, or ϕ tends to 0 or 1, constant amplitude conditions are approached and γ tends to 1.

The results of Gurney [20] bear a striking resemblance to those of the present study. In particular, Gurney found a similar dependence of γ upon ϕ, compare Figs 5 and 9.

In order to examine the range in loading over which accelerated growth takes place, three further tests were conducted on 3 mm thick BS 4360 50B material:

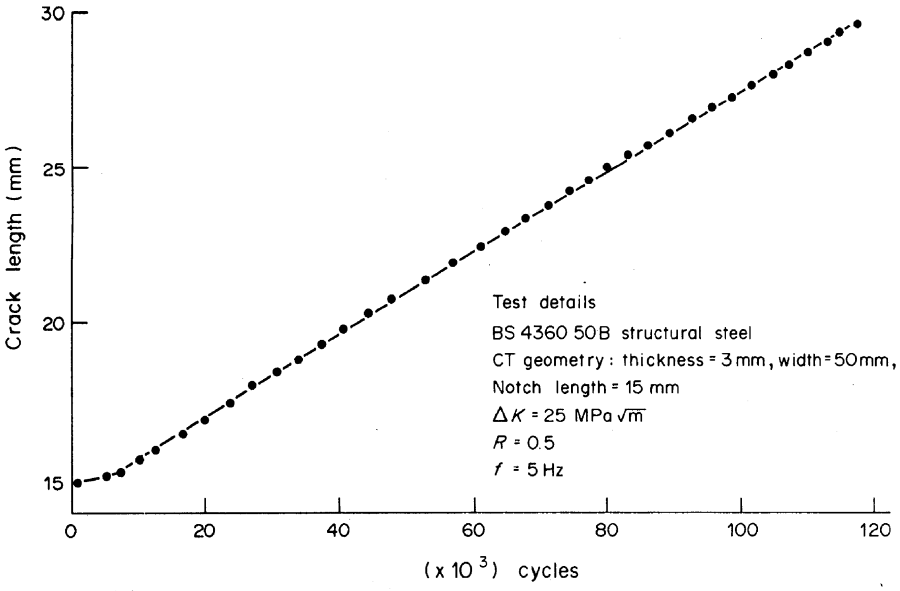

Fig. 7. Typical plot of crack length against number of fatigue cycles.

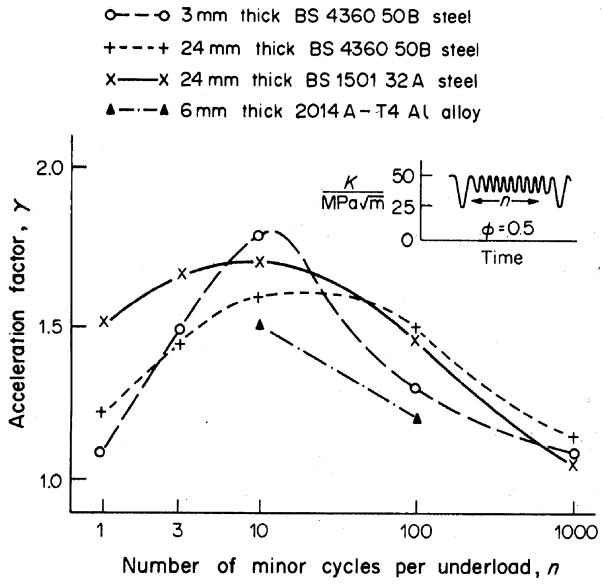

Fig. 8. Acceleration effect due to periodic underloads. Acceleration factor, γ, vs number of minor cycles, n.

(a) A specimen was fatigued at a load ratio, R, of 0.5 and constant load range, such that ΔK at the start of the test was 14 MPa$\sqrt{\text{m}}$ while ΔK at the end of the test was 30 MPa$\sqrt{\text{m}}$.

(b) A specimen was fatigued at a load ratio, R, of 0.75 and constant load range, such that ΔK rose from 7 MPa$\sqrt{\text{m}}$ at the start to 15 MPa$\sqrt{\text{m}}$ at the end of the test.

(c) A specimen was fatigued with periodic underloads, such that $n = 10$ and $\phi = 0.5$, see Fig. 10. The load ratio of the major cycles, that is the underloads, was 0.5. No load shedding scheme was employed. At the start of the test the stress intensity range for the major cycles, ΔK_{major}, was 14 MPa$\sqrt{\text{m}}$, while at the end of the test ΔK_{major} was 30 MPa$\sqrt{\text{m}}$.

The measured crack growth rates due to the load sequences (a)–(c) are given in Fig. 10. Predicted growth rates for load sequence (c) result from a linear

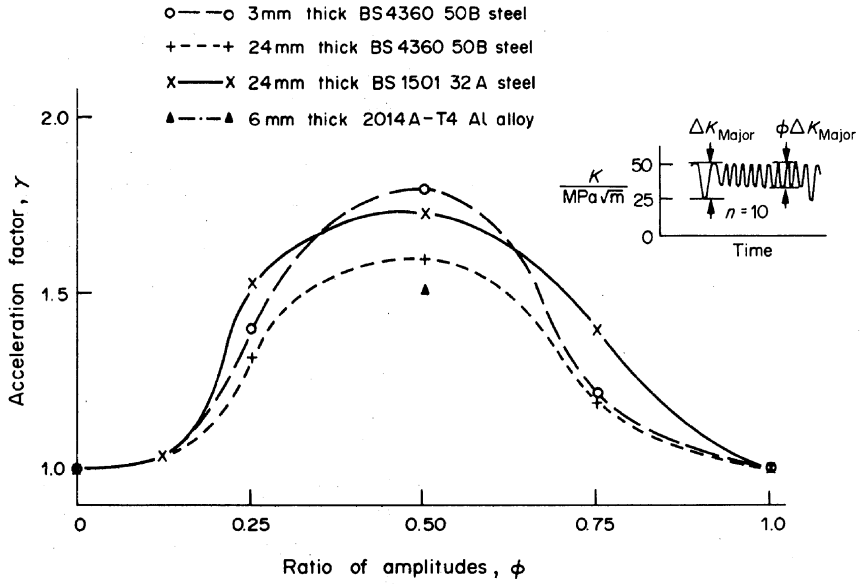

Fig. 9. Acceleration effect due to periodic underloads. Acceleration factor, γ, vs ratio of amplitudes, ϕ.

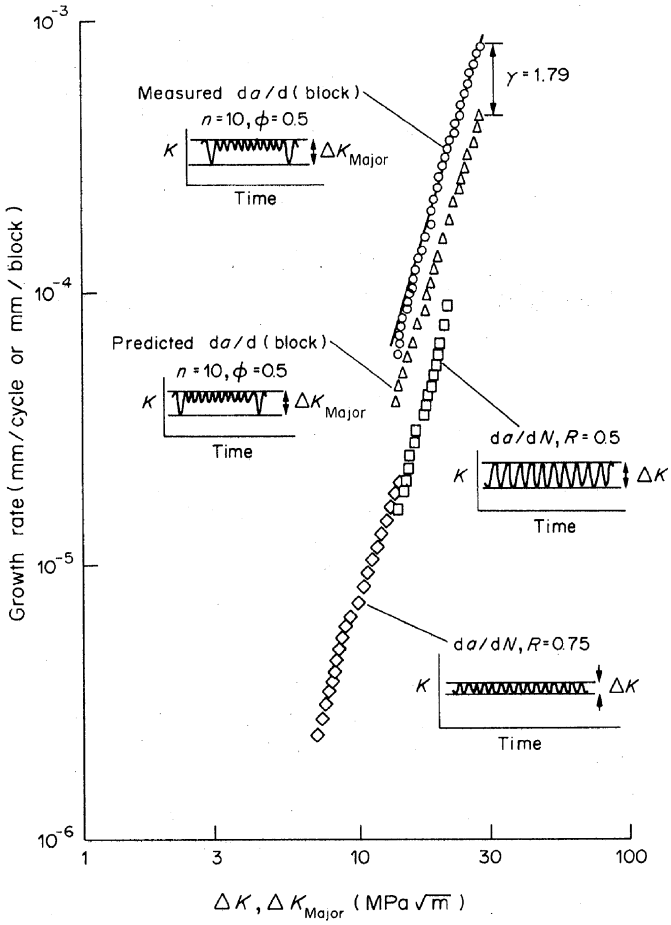

Fig. 10. Comparison of measured and predicted growth rates for ΔK_{major} in the range 14–30 MPa$\sqrt{m}$. Periodic underloads, $n = 10$, $\phi = 0.5$. 3 mm thick BS4360 50B steel.

summation of the growth rates from tests (a) and (b); predicted growth rates are included in Fig. 10.

Periodic underloads cause a fatigue crack to propagate 80% faster than predicted by linear summation, for ΔK_{major} in the range 17 MPa$\sqrt{m}$ to 30 MPa$\sqrt{m}$, see Fig. 10. As near threshold growth is approached, such that ΔK_{major} is less than 17 MPa$\sqrt{m}$, the acceleration factor is reduced.

Periodic overloads

The effect of varying the number of small cycles, n, per overload upon crack growth rate is given in Table 2 and Fig. 11. Tests were conducted on 24 mm thick BS4360 50B and BS1501 32A steel specimens.

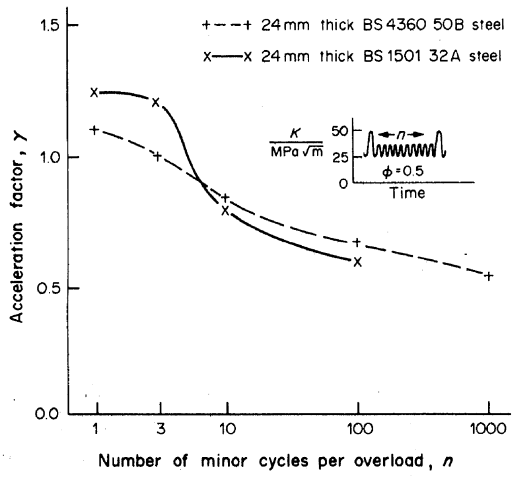

Fig. 11. Acceleration effect due to periodic overloads. Acceleration factor, γ, vs number of minor cycles, n.

The acceleration factor, γ, decreases monotonically from about 1.2 to 0.6, as n is increased from 1 to 1000, for both materials. Crack growth rates are accelerated for n less than or equal to 3 and retarded for n greater than 3.

MECHANISMS CAUSING ACCELERATED AND RETARDED GROWTH

Cycle counting routines such as rainflow [23–25], level crossing [26], range mean [25] and racetrack [25, 27] are often used to account for fatigue load interaction effects. The rainflow technique has become very popular since it is able to identify the closed stress-strain hysteresis loops experienced by material at a notch or crack tip, due to the applied load sequence. Often, use is made of rainflow counting, crack closure arguments and a Miner-type linear summation of damage to account for crack growth due to variable amplitude loading [28, 29].

We cannot use cycle counting methods to explain accelerated and retarted growth due to periodic overloads and underloads: each counting technique predicts the same response. Instead we must appeal to physical mechanisms by which cracks grow faster or slower than the constant amplitude growth rate, see Table 3. Since the growth rates recorded in this study are far above threshold, the mechanisms causing the accelerated and retarded growth may differ significantly from those operative near threshold [30]. Several mechanisms may be operative simultaneously; experimental evidence indicates that many are not operative. Each will be discussed in turn.

1. *Crack closure*

Crack closure arguments successfully account for the severe retardations which follow application of a single peak overload to BS4360 50B steel [3, 31]. Can the same arguments be used to explain the present results?

Crack mouth, crack tip and back face compliance measurements indicated that the crack was held open for the whole of the fatigue cycle, for all periodic overload, periodic underload and associated constant amplitude tests. It is concluded that the crack closure phenomenon and associated closure models [32–34] are unable to account for the accelerated or retarded growth shown in this study.

2. *Crack tip sharpening/blunting*

Consider first periodic underloads. If the underloads were able to sharpen the crack tip so that faster growth accompanied the minor cycles, then an acceleration effect would result. A plastic replication technique [22] was employed to test this hypothesis.

Periodic underloads were applied to a 3 mm thick BS4360 50B specimen, such that $n = 10$, and $\phi = 0.5$. Crack tip replicas were taken at each turning value of a single load block. Examination of the replicas in the

Table 2. Results of constant amplitude, periodic underload and periodic overload tests

Constant amplitude response, steels

ΔK (MPa$\sqrt{\text{m}}$)	Load ratio, R	Crack growth rate, $\frac{da}{dN}$, (mm/cycle) 3 mm thick BS4360 50B Steel	24 mm thick BS4360 50B Steel	24 mm thick BS1501 32A Steel
25	0.5	1.21×10^{-4}	1.34×10^{-4}	1.19×10^{-4}
12.5	0.75	1.16×10^{-5}	1.28×10^{-5}	1.45×10^{-5}
12.5	0.667	—	1.72×10^{-5}	1.42×10^{-5}
18.75	0.625	4.31×10^{-5}	4.77×10^{-5}	4.37×10^{-5}
6.25	0.875	1.86×10^{-6}	1.90×10^{-6}	1.89×10^{-6}
3.13	0.938	—	—	2.50×10^{-7}

Constant amplitude response, 6 mm thick 2014A-T4 Al alloy specimens

ΔK (MPa$\sqrt{\text{m}}$)	Load ratio, R	$\frac{da}{dN}$ (mm/cycle)
8.0	0.5	1.19×10^{-4}
4.0	0.75	4.70×10^{-6}

Periodic underloads, $\phi = 0.5$

Number of minor cycles per underload, n	Crack growth per block (mm/block) 3 mm thick BS4360 50B steel	24 mm thick BS4360 50B steel	24 mm thick BS1501 32A steel	6 mm thick 2014A-T4 Al alloy	Acceleration factor, γ 3 mm thick BS4360 50B steel	24 mm thick BS4360 50B steel	24 mm thick BS1501 32A steel	6 mm thick 2014A-T4 Al alloy
1	1.44×10^{-4}	1.79×10^{-4}	2.02×10^{-4}	—	1.09	1.22	1.51	—
3	2.31×10^{-4}	2.49×10^{-4}	2.71×10^{-4}	—	1.49	1.45	1.66	—
10	4.23×10^{-4}	4.18×10^{-4}	4.55×10^{-4}	2.51×10^{-4}	1.79	1.60	1.72	1.51
100	1.66×10^{-3}	2.12×10^{-3}	2.29×10^{-3}	7.10×10^{-4}	1.30	1.50	1.46	1.20
1000	1.27×10^{-2}	1.47×10^{-2}	1.57×10^{-2}	—	1.09	1.14	1.07	—

Periodic underloads, $n = 10$

Ratio of amplitudes, ϕ	Crack growth per block (mm/block) 3 mm thick BS4360 50B steel	24 mm thick BS4360 50B steel	24 mm thick BS1501 32A steel	6 mm thick 2014A-T4 Al alloy	Acceleration factor, γ 3 mm thick BS4360 50B steel	24 mm thick BS4360 50B steel	24 mm thick BS1501 32A steel	6 mm thick 2014A-T4 Al alloy
0.125	—	—	1.25×10^{-4}	—	—	—	1.03	—
0.25	1.94×10^{-4}	2.01×10^{-4}	2.10×10^{-4}	—	1.39	1.32	1.52	—
0.50	4.23×10^{-4}	4.18×10^{-4}	4.55×10^{-4}	2.51×10^{-4}	1.79	1.60	1.72	1.51
0.75	6.66×10^{-4}	7.28×10^{-4}	7.56×10^{-4}	—	1.21	1.19	1.36	—

Periodic overloads, $\phi = 0.5$

Number of minor cycles per overload, n	Crack growth per block (mm/block) 24 mm thick BS4360 50B steel	24 mm thick BS1501 32A steel	Acceleration factor, γ 24 mm thick BS4360 50B steel	24 mm thick BS1501 32A steel
1	1.62×10^{-4}	1.65×10^{-4}	1.11	1.24
3	1.73×10^{-4}	1.94×10^{-4}	1.01	1.20
10	2.17×10^{-4}	2.09×10^{-4}	0.84	0.80
100	9.27×10^{-4}	9.23×10^{-4}	0.67	0.60
1000	6.95×10^{-3}	—	0.55	—

scanning electron microscope showed that the underload slightly blunted rather than sharpened the crack tip. We assume that such blunting retards growth and conclude that other mechanisms must be used to explain the acceleration effect.

For the case of periodic overloads, it is thought that blunting of the crack tip accompanies each overload in the same manner that a single peak overload causes crack tip blunting [16]. Since retardation only occurs when more than 3 minor cycles follow each periodic overload, this cannot be the sole mechanism in operation.

3. *Crack tip branching*

The stress intensity at the tip of a branched crack is less than that at the tip of a straight crack [35]. Hence, if variable amplitude loading causes the crack path to be highly deviated, retardation will ensue.

Table 3. Possible mechanisms causing accelerated and retarded growth

Phenomena	Acelerated growth due to periodic underloads	Accelerated growth due to periodic overloads ($n \leqq 3$)	Retarded growth due to periodic overloads ($n > 3$)
Materials investigated	BS4360 50B and BS1501 32A steels Al 2014A-T4	BS4360 50B and BS1501 32A steels	BS4360 50B and BS1501 32A steels
Possible mechanisms			
(1) Crack closure	×	×	×
(2) Crack tip sharpening or blunting	×	×	√
(3) Crack tip branching	×	×	×
(4) Strain hardening of material ahead of the crack tip due to the major cycles	√	√	×
(5) Change in rate of damage accumulation in the reversed plastic zone ahead of the crack tip	×	×	×
(6) Cyclic hardening or softening in the reversed plastic zone ahead of the crack tip	×	×	×
(7) Change in the crack growth mechanism and dislocation structure near the crack tip, due to the major cycles	×	×	×
(8) Influence of mean stress on the crack growth mechanism	√	×	√

√—may be operative.
× —discounted.

Bucci *et al* [36] have applied periodic overloads to several aluminium alloys of the 7000 series. The ratio, ϕ, was 0.55 and the number, n, was 4000 and 8000 for these tests. Bucci *et al.* found greatest retardations in low purity 7075–T6 aluminium alloys and least retardations in high purity 7050-T7 and 7475-T7 aluminium alloys. They also observed that fissures and numerous secondary cracks were typical at overload sites in the low purity material, but not in the high purity materials. It was concluded that crack branching led to the retarded growth in both high and low purity materials; this branching was encouraged by the presence of secondary intermetallic particles.

At present, there is dispute over the ability of crack branching to account for retardation after single peak overloads. Recent work [3] has shown that crack growth retardation following a single peak overload in thick and thin specimens made from BS4360 50B steel is due to plasticity-induced crack closure rather than crack branching. On application of an overload, crack growth rates in thick test-pieces decreased from 10^{-4} to 10^{-5} mm/cycle, with no evidence of crack branching. Small deviations in crack path were observed when thin specimens were subjected to single peak overloads, but no correlation was found between either size or location of these deviations and the crack growth rate transients.

Lankford and Davidson [37] have provided further evidence to suggest that retardation following a single peak overload is not due to crack tip branching. They applied single peak overloads to 7075-T6, 2024-T4 and 6061-T6 aluminium alloys; tests were performed in a scanning electron microscope using a special loading stage. Lankford and Davidson observed that crack tip branching after the overload led to an initial *acceleration* in crack growth rate. Retardation occurred only after the fatigue crack had grown out of the influence of the branch and had re-oriented itself normal to the loading axis.

It seems that crack tip branching is not the cause of crack growth retardation after a single peak overload, but may enhance the retardation when growth rates are near threshold and crack advance is crystallographic in nature [3, 30, 38].

In order to determine whether crack branching occurred in the periodic overload and periodic underload tests of the present study, metallographic sections were taken normal to the thickness direction and at mid-plane of the thick BS4360 50B steel specimens, see Fig. 12. The crack path was highly tortuous and secondary cracks were apparent in every case. The degree of crack branching for the case of periodic overloads ($n = 1000$, $\phi = 0.5$) was comparable with that due to applying only the minor cycles. It is concluded that crack tip branching is not the cause of retarded growth in BS4360 50B steel subjected to periodic overloads.

The fracture surface produced by periodic underloads ($n = 10$, $\phi = 0.5$) was also examined, Fig. 12.

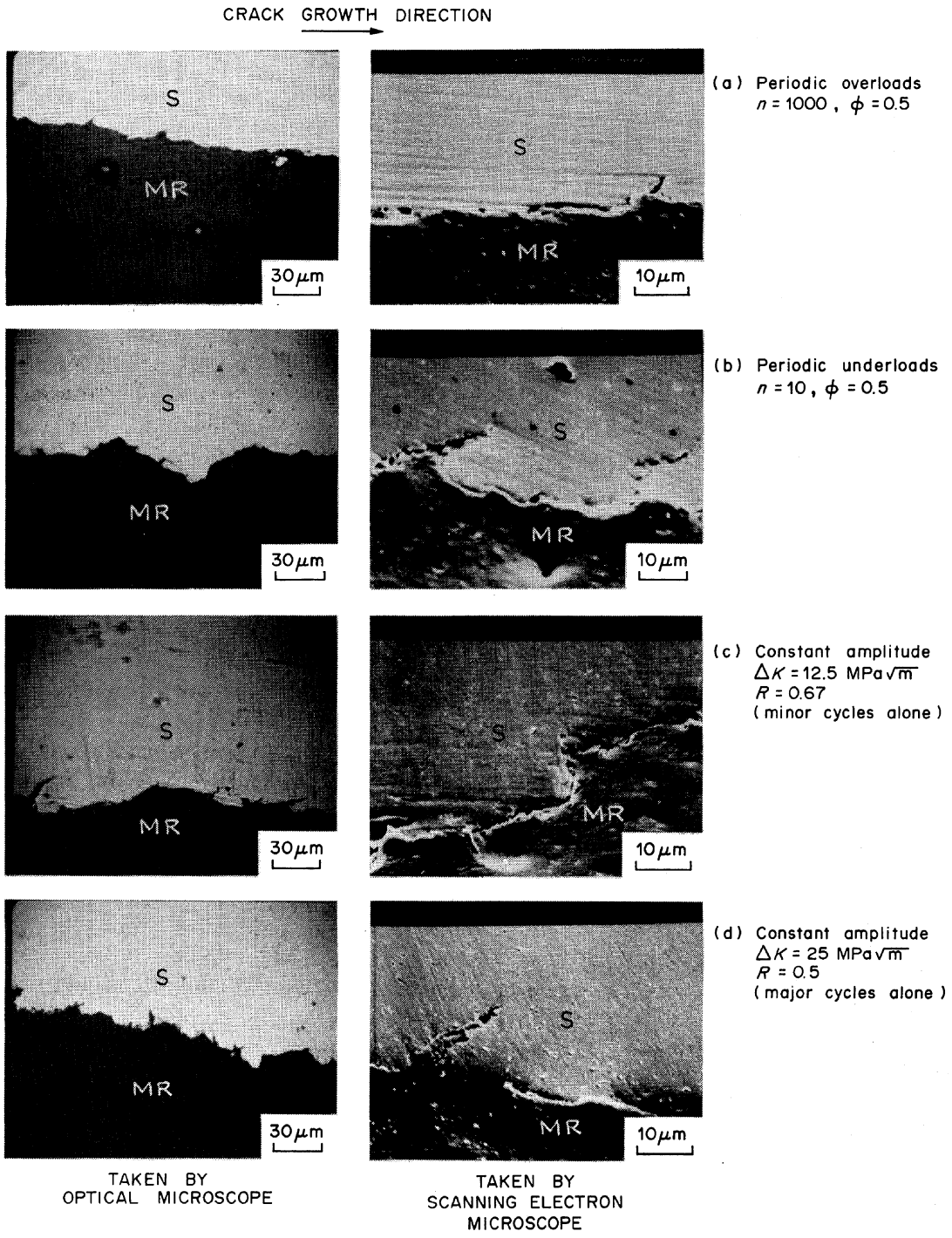

Fig. 12. Sections of the fatigue fracture surfaces to show that branching does not lead to retarded or accelerated growth in thick BS4360 50B steel specimens. In each micrograph, S marks the steel specimen and MR designates the mounting resin.

Since the degree of crack branching was again comparable with that due to applying only the minor cycles, it is deduced that accelerated growth is not caused by a reduction in the amount of crack branching.

These conditions probably apply also to BS1501 32A steel since it is similar in microstructure, composition and strength to BS4360 50B steel. No periodic overload tests were performed on the 2014A-T4 aluminium alloy.

4. *Strain hardening of material at crack tip*

Schijve [39] has investigated the effect of 3% prestrain upon the crack propagation response of 2024–T3 aluminium alloy. Fatigue cracks grew twice as quickly in the strain hardened material as in the as-received material. It was concluded that about half of the acceleration effect was due to the crack closure phenomenon and half due to a reduction in material ductility by strain hardening.

In the field of low cycle fatigue, it is well established that fatigue life is reduced by strain hardening a specimen at the start of the test, for example [40].

In the present study, a strain hardening argument would suggest that faster crack growth accompanies the minor cycles after an underload or overload. The fracture surfaces of several specimens were examined to support or refute this suggestion. Clearly defined

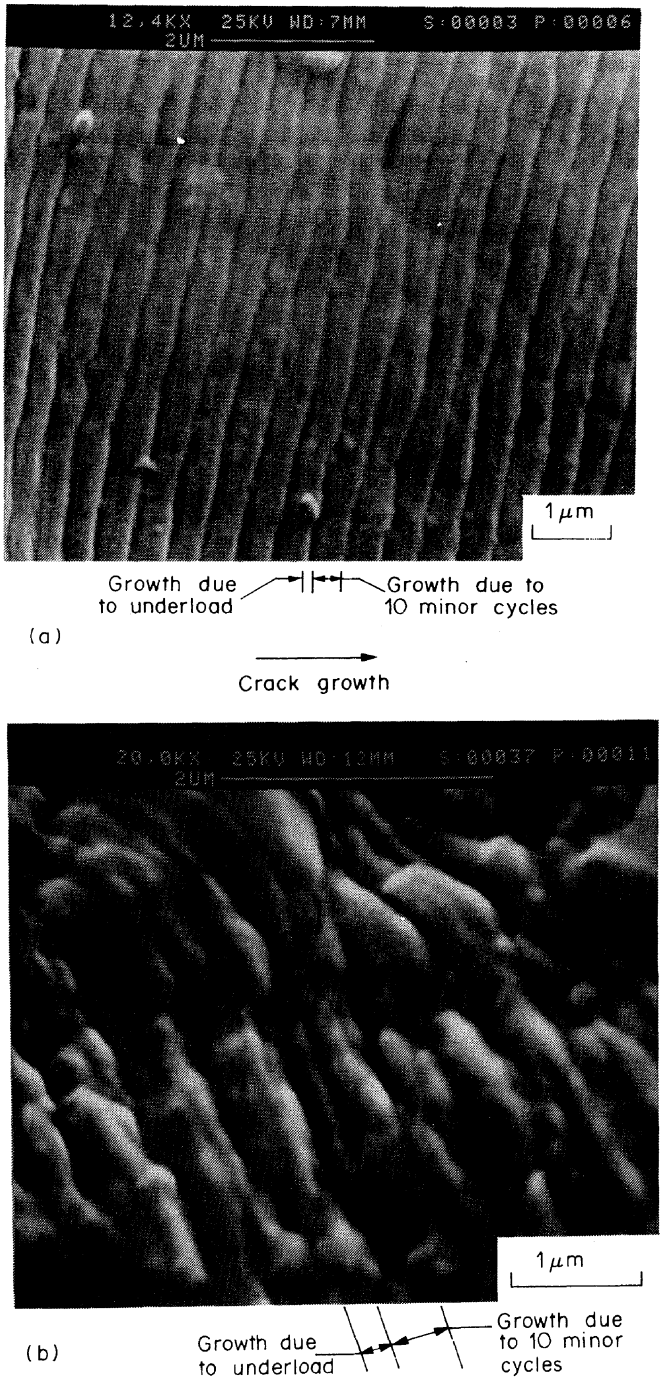

Fig. 13. (a) Fracture surface of 6 mm thick 2014A-T4 aluminium alloy specimen, due to periodic underloads. $n = 10$, $\phi = 0.5$. (b) Fracture surface of 3 mm thick BS4360 50B steel specimen, due to periodic underloads. $n = 10$, $\phi = 0.5$.

striations were observed for the aluminium alloy, but in the steels only poorly defined striations were seen. It was found that faster or slower growth arose from larger or smaller crack growth increments associated with the minor cycles, rather than the underloads or overloads, Fig. 13.

McMillan and Pelloux [11] have published fractographs for 2024-T3 aluminium alloy subjected to the programmed loading of Fig. 1(b). Careful measurement of striation spacings shows that faster growth accompanied the small amplitude cycles. Thus, the strain hardening argument finds further support.

From the observation that the crack growth increment accompanying each underload and overload was similar for all tests, we may deduce the crack growth increment accompanying each minor cycle. For instance, consider periodic underloads, with $\phi = 0.5$. The crack growth increment for 1 underload and 10 minor cycles ($n = 10$) is Δa_{10}, while the crack growth increment for 1 underload and 100 minor cycles ($n = 100$) is Δa_{100}. It is deduced that the average crack growth rate for the 11th to 100th cycle of the latter load sequence is $(\Delta a_{100} - \Delta a_{10})/90$. We may plot this average growth rate against the average minor cycle number, $(100 + 10)/2$. Results of this procedure for both the periodic overloads and periodic underloads are shown in Fig. 14, using the data of Table 2.

The general trend of Fig. 14 is a gradually decreasing growth rate accompanying each subsequent minor cycle. For the periodic underload tests, accelerated growth accompanies each minor cycle and the strain hardening argument is supported. In the case of periodic overloads, provided that 3 or less minor cycles are applied for each overload, accelerated growth accompanies the minor cycles. However, for a large number of minor cycles per overload, the crack growth increment accompanying each minor cycle is reduced to below the constant amplitude value, and retardation dominates. It is clear that strain hardening arguments alone are unable to explain the periodic overload results.

Broek and Leis [10] have used similar arguments to explain accelerated growth in 7075-T6 aluminium alloy when subjected to programmed loading akin to periodic overloads and underloads, see Figs 1(a) and 3.

5. *Change in rate of damage accumulation in the reversed plastic zone*

Several authors, for example [41–43], have suggested that crack advance is a result of damage accumulation due to reversed plasticity ahead of the crack tip. If so, then the load interaction effects observed in low cycle fatigue tests on plain specimens may be used to account for accelerated and retarded crack growth.

Kikukawa *et al.* [44] have tested plain specimens made from JIS S35C steel, using periodic underloads and periodic overloads. They applied 98 minor cycles ($n = 98$) for each underload or overload; each minor cycle was half the amplitude of the major cycle ($\phi = 0.5$). It was found that periodic underloads gave rise to fatigue lives an order of magnitude shorter than periodic overloads. Since JIS S35C steel has similar tensile properties to BS4360 50B steel, we may compare their results with those of the present study.

Consider the cases of periodic overloads and periodic underloads applied to 24 mm thick BS4360 50B and BS1501 32A steel specimens, with $n = 100$ and $\phi = 0.5$. The fatigue life due to periodic underloads

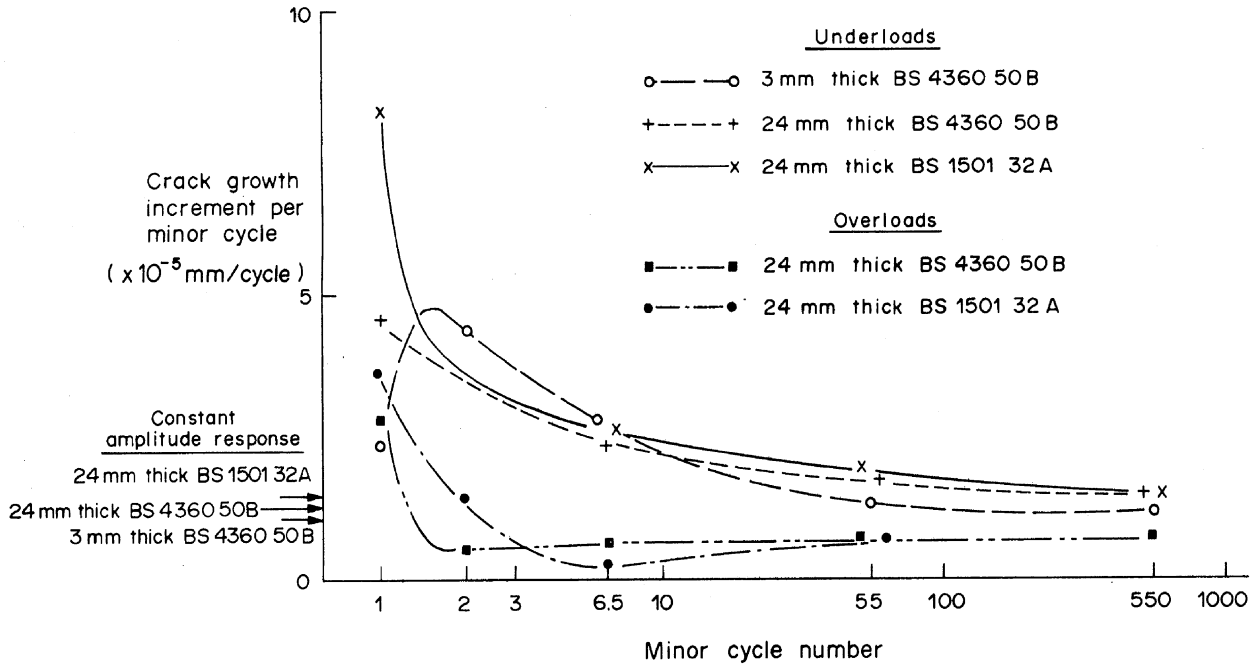

Fig. 14. Crack growth rate per minor cycle, assuming that the major cycle crack growth increment is unaffected by the load sequence.

was half that due to periodic overloads for both steels, see Figs 8 and 11. Since the fatigue loads employed by Kikukawa *et al.* were much closer to the fatigue limit than in the present study, we might expect them to have observed a larger acceleration effect, which is indeed the case [44].

There is much evidence that fatigue crack advance is governed by cyclic crack openings at the crack tip, rather than damage accumulation ahead of the crack tip due to reversed plasticity [45–47]. Further, there is a lack of similitude between a fatigue crack tip plastic zone and a plain specimen. Unlike a plain specimen, a crack tip plastic zone is a region of high strain gradient and possibly plastic constraint. Consequently, any similarity between load interaction effects revealed by low cycle fatigue tests and by crack growth tests may be purely fortuitous. This is evidenced by the fact that a single peak overload decreases the fatigue life of a plain specimen but increases the crack propagation life of a conventional LEFM test-piece.

6. *Cyclic hardening or softening in reversed plastic zone*

Crack growth delay following a single peak overload increases with the rate at which a material cyclically hardens [48]. Cyclic stress–strain tests have been performed on BS4360 43A structural steel [49]; this material is similar in composition and properties to the BS4360 50B steel. It was found that the 43A material was cyclically stable: its cyclic and monotonic strengths were comparable. Hence, we cannot appeal to a cyclic hardening or softening argument to explain the accelerated and retarded growth of the present study.

7. *Change in crack growth mechanism and dislocation structure*

Koterazawa [15] has explained accelerated growth due to periodic overloads in terms of a change in crack growth mechanism from striation-forming to a zig-zag mode, in association with the development of a radial dislocation structure near the crack tip. He considered a variety of steels and limited his investigation to near threshold growth (about 10^{-7} mm/cycle).

In the present study, crack growth rates were far above threshold. The crack advance mechanism for both constant amplitude and programmed loading produced striations. Thus the observed load interaction effects were not due to the mechanism proposed by Koterazawa.

8. *Influence of mean stress on crack growth mechanism*

It is well known that mean stress relaxation occurs in the reversed plastic sone near a crack tip, under constant amplitude loading [50, 51]. The crack tip experiences fully reversed loading even when the applied loading is tensile–tensile.

When periodic overloads or underloads are applied to a specimen, it is likely that the mean stress of the major cycles relaxes to zero, but not the mean stress of the minor cycles, Fig. 15. The minor cycles associated with periodic underloads have a tensile mean stress, while the minor cycles associated with periodic overloads have a compressive mean stress. Little is known about the influence of mean stress on the striation crack growth mechanism, but it seems plausible that tensile mean stresses will lead to faster growth and compressive mean stresses to slower growth.

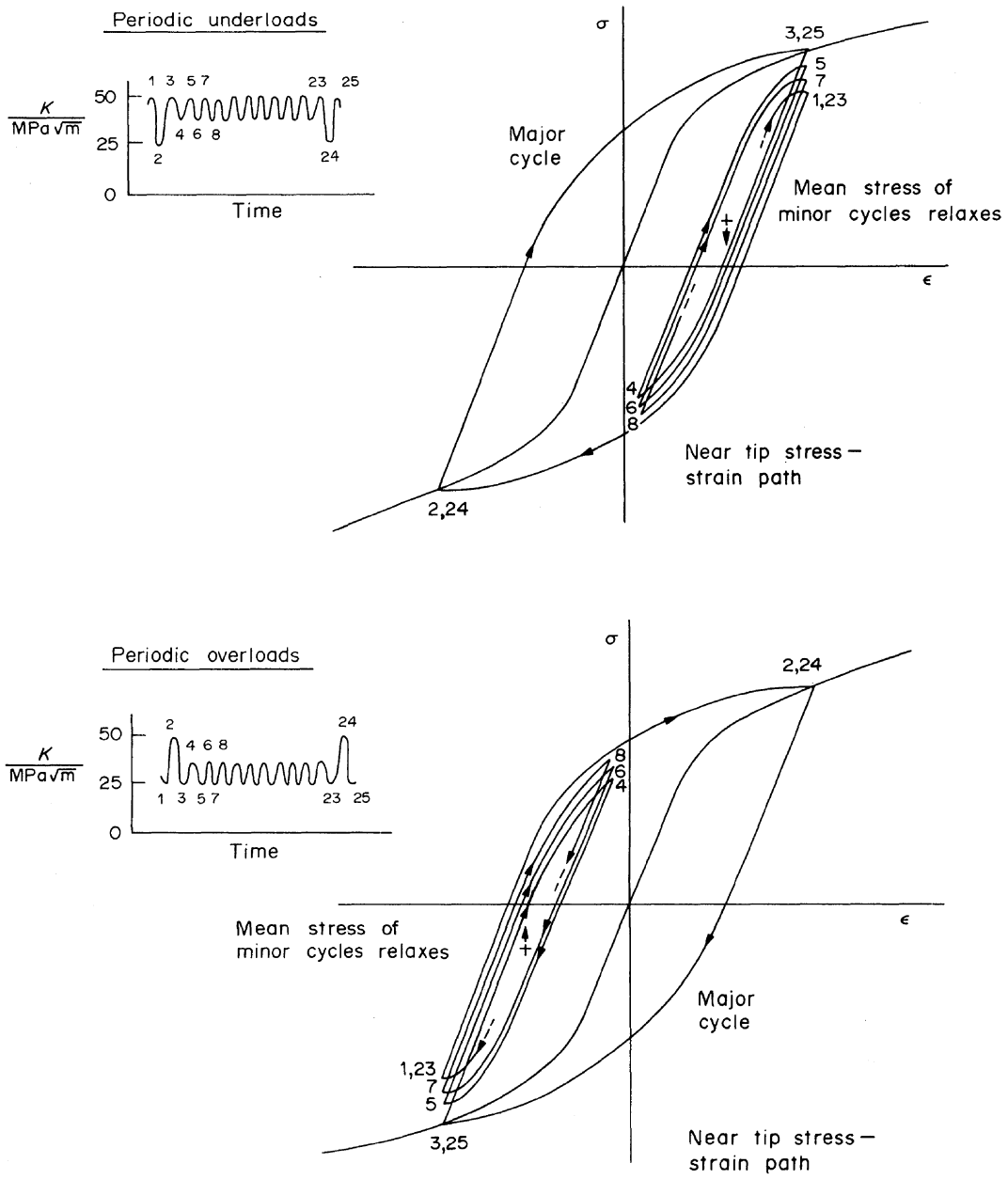

Fig. 15. Possible control conditions at crack tip

The phenomenon of mean stress relaxation [52] is also depicted in Fig. 15. By this mechanism, the mean stress of succeeding minor cycles gradually approaches zero until the next underload or overload re-establishes an extreme mean stress. The expected crack advance per minor cycle agrees with the trends given in Fig. 14. If no more major cycles were applied, the stress–strain loop at the crack tip would revert to the state characteristic of constant amplitude loading. In other words, the mean stress would relax to zero.

The exact control condition at the crack is not known—it may be strain control where $\Delta\varepsilon = f(\Delta K)$ [43], or Neuber control where $\Delta\sigma \cdot \Delta\varepsilon = f(\Delta K)$ [42]. Whatever is the control condition, the above arguments apply.

Mean stresses relax much less quickly in plain specimens made from aluminium alloys than plain specimens made from steels, for the same cyclic plastic strain range [52]. Thus, when subjected to periodic underloads, aluminium alloys should show greater acceleration effects than low strength steels. Unfortunately, the opposite is true, see Fig. 8. This observation, together with the fact that periodic overloads followed by 3 or less minor cycles give accelerated growth, implies that mean stress relaxation is not the sole mechanism in operation.

Conventional retardation models of Wheeler and Willenborg et al.

Wheeler [53] and Willenborg *et al.* [54] have proposed quantitative models to account for crack growth retardation following a single peak overload. The models are based on the assumption that material ahead of the crack tip experiences compressive stresses due to the overload. A brief description of the models is given in Appendix I.

The predictions of the Wheeler and Willenborg *et al.* models are compared with measured growth rates for the case of periodic overloads, Fig. 16. It is widely

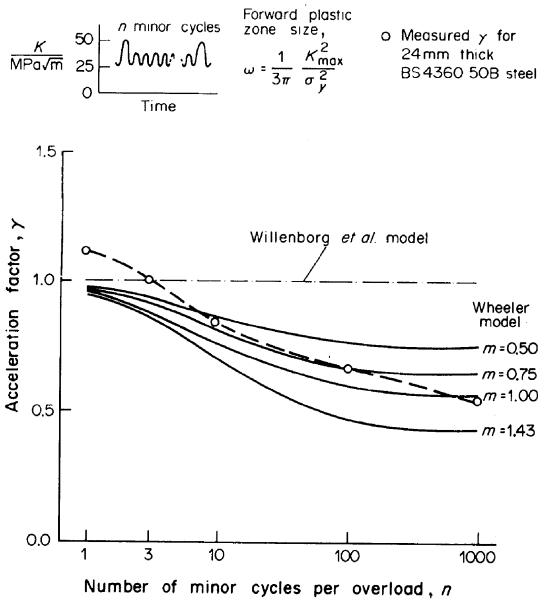

Fig. 16. Accuracy of the models of Wheeler [53] and Willenborg *et al.* [54]. Periodic overloads, $\phi = 0.5$.

accepted [26] that the Wheeler index, m, has to be adjusted for different materials and classes of waveform in order to give maximum predictive accuracy. For the case of periodic overloads applied to BS4360 50B steel, Wheeler's model predicts crack growth rates to an accuracy of $\pm 20\%$ for $m = 0.75$, Fig. 16. The Willenborg *et al.* model predicts no load interaction effect for periodic overloads, since a high mean stress is present, Fig. 16. Neither model is able to give accelerated growth: both erroneously predict $\gamma = 1$ for all periodic underload tests.

It is concluded that accelerated and retarded growth may be due partly to a mean stress influence on the crack advance mechanism. Wheeler's model can be used with some success to predict retarded growth due to periodic overloads, but cannot predict accelerated growth associated with periodic underloads. The model of Willenborg *et al.* fails to account for the load interaction effects which accompany periodic underloads and periodic overloads.

Summary of mechanisms

The mechanisms which give rise to accelerated and retarded growth are listed in Table 3. These mechanisms are not totally independent of each other. For instance, crack tip blunting is inevitably accompanied by strain hardening of material at the crack tip. The mechanisms which give rise to the accelerated and retarded growth of the present study may, however, be resolved. The accelerated growth which accompanies periodic underloads is probably due to strain hardening and to mean stress effects. Similarly, the accelerated growth accompanying periodic overloads ($n \leqq 3$) results from strain hardening at the crack tip.

When more than 3 minor cycles follow each periodic overload, retardation dominates. Retardation is caused by a combination of blunting and mean stress effects.

CONCLUSIONS

Periodic underloads and periodic overloads have been applied to fatigue specimens made from BS4360 50B structural steel, BS1501 32A pressure vessel steel and 2014A-T4 aluminium alloy. The loading was of sufficient magnitude to cause fatigue cracks to grow at rates typical of the mid-regime of the Paris plot. For such test conditions the following conclusions may be drawn:

(1) Periodic underloads cause faster growth than that predicted by a linear summation of the constant amplitude crack growth response. Measured growth rates are nearly twice those predicted, for the case of 10 small cycles per underload, with each small cycle half the amplitude of the underload. Such accelerated growth is not influenced by a change of material or stress state.

(2) Periodic overloads, consisting of up to 3 small cycles followed by an overload, lead to faster growth by up to 20%. When more than 3 small cycles are applied per overload, retardation results.

(3) Load interaction phenomena due to periodic underloads and periodic overloads cannot be explained by cycle counting techniques, or by crack closure arguments. A number of alternative mechanisms may operate simultaneously and lead to the accelerated and retarded growth. These mechanisms are crack tip blunting, strain hardening and mean stress effects.

Acknowledgements—The author wishes to thank the Director of British Gas Engineering Station for the provision of test materials and equipment, and Dr R. A. Smith and Mr M. C. Smith for helpful discussions. British Gas originally suggested that underloads could accelerate fatigue crack growth rates. The author is grateful to Pembroke College for financial support in the form of a Maudslay Research Fellowship.

REFERENCES

1. W. Elber, *ASTM STP* **486,** 230 (1971).
2. P. C. Paris and L. Hermann, *1st Int. Symp. on Fatigue Thresholds*, Stockholm (edited by J. Bäcklund, A. F. Blom and C. J. Beevers), Vol. 1. p. 3 EMAS, Warley, U.K. 3 (1982).
3. N. A. Fleck, *ASTM-1984 Workshop and Symposium on Fundamental Questions and Critical Experiments on Fatigue*, Dallas, Texas, October (1984).
4. N. A. Fleck and R. A. Smith, *Seeco '83—Digital Techniques in Fatigue*, London (edited by B. J. Dabell), pp. 190–196. Soc. Environ. Engnrs (1983).
5. N. A. Fleck and R. A. Smith, *Sixth Int. Conf. on Fracture*, Delhi (1984).
6. D. G. Jones, private communication (1980).
7. B. E. Powell, T. V. Duggan and R. Jeal, *Int. J. Fatigue* **4,** 4 (1982).
8. D. Broek and R. C. Rice, *Natn. SAMPTE Tech. Conf. Ser.* **9,** 392 (1977).
9. J. Schijve, *Engng Fract. Mech.* **11,** 167–221 (1979).

10. D. Broek and B. N. Leis, *Proc. Fatigue '81, SEE Fatigue Group Conf.* Warwick Univ., England (edited by F. Sherratt and J. B. Sturgeon), pp. 129–146. Westbury, Guildford, England (1981).
11. J. C. McMillan and R. M. N. Pelloux, *ASTM STP* **415,** 505 (1967).
12. H. Nowack, K. H. Trautmann, K. Schulte and G. Lütjering, *ASTM STP* **677,** 36 (1979).
13. V. W. Trebules, R. Roberts and R. W. Hertzberg, *ASTM STP* **536,** 115 (1973).
14. R. W. Hertzberg, *Deformation and Fracture Mechanics of Engineering Materials*, 2nd edn. Wiley, New York (1983).
15. R. Koterazawa, *Proc. Fatigue '81, SEE Fatigue Group Conf.* Warwick Univ., England (edited by F. Sherratt and J. B. Sturgeon), pp. 159–169. Westbury House, Guildford, England (1981).
16. H. Kobayashi, H. Nakamura, A. Hirano and H. Nakazawa, *Proc. of Fatigue '81, SEE Fatigue Group Conf.*, Warwick Univ, England (edited by F. Sherratt and J. B. Sturgeon, pp. 318–327. Westbury House, Guildford, England (1981).
17. H. Nisitani and K. Takao, *Engng Fract. Mech.* **10,** 855 (1978).
18. M. Kikukawa, M. Jono and Y. Kondo, *Advances in Fracture Research, ICF5*, Cannes (edited by D. Francois), pp. 1799–1806. Pergamon Press, Oxford (1981).
19. S. Suresh and R. O. Ritchie, *Mater. Sci. Engng* **51,** 61 (1981).
20. T. R. Gurney, *Proc. R. Soc. Lond.* **A386,** 393 (1983).
21. N. A. Fleck and T. Hooley, *Seeco '83—Digital Techniques in Fatigue*, London (edited by B. J. Dabell), pp. 309–316. Soc. Environ. Engrs (1983).
22. N. A. Fleck, Cambr. Univ. Engng Depart. Rep. CUED/C/MATS/TR. 89 (1982).
23. M. Matsuishi and T. Endo, *Japan Soc. Mech. Engrs*, Japan (1968).
24. S. D. Downing and D. F. Socie, *Int. J. Fatigue* **4,** 31 (1982).
25. H. O. Fuchs and R. I. Stephens, *Metal Fatigue in Engineering*. Wiley, New York (1980).
26. D. Broek, *Elementary Engineering Fracture Mechanics*, 3rd edn. Martinus Nijhoff Publishers, The Netherlands (1982).
27. A. Teichmann, *The Strain Range Counter*. Vickers-Armstrong Aircraft Ltd., Tech. Office, VTO/M/46 (1955).
28. D. F. Socie, *Engng Fract. Mech.* **9,** 849 (1977).
29. M. Kikukawa, M. Jono and S. Mikami, *J. Soc. Mater. Sci., Japan* **31,** 483 (1982).
30. S. Suresh, *Engng Fract. Mech.* **18,** 577 (1983).
31. N. A. Fleck, I. F. C. Smith and R. A., Smith, *Fatigue Engng Mater. Struct.* **6,** 225 (1983).
32. A. U. de Koning, *Fracture Mechanics: Thirteenth Conf.* (edited by R. Roberts), ASTM STP 743, pp. 63–85 (1980).
33. H. Führing, *Advantages in Fracture Research, ICF5*, Cannes (Edited by D. Francois), Vol. 4, pp. 1823–1832. Pergamon Press, Oxford (1981).
34. J. C. Newman Jr, *ASTM STP* **748,** 53 (1981).
35. B. A. Bilby, G. E. Cardew and I. C. Howards, *Fracture 1977* (edited by D. M. R. Taplin), Vol. 3, pp. 197–200. Univ. of Waterloo Press (1977).
36. R. J. Bucci, A. B. Thakker, T. H. Sanders, R. R. Sawtell and J. T. Staley, *ASTM STP* **714,** 41 (1980).
37. J. Lankford and D. L. Davidson, *Advances in Fracture Research* (edited by D. Francois *et al.*), Vol. 2, 899–906. Pergamon Press, Oxford (1981).
38. R. S. Vecchio, R. W. Hertzberg and R. Jaccard, *Fatigue Engng Mater. Struct.* **7,** 181 (1984).
39. J. Schijve, *Engng Fract. Mech.* **8,** 575 (1976).
40. L. Legris, M. H. El Haddad and T. H. Topper, *Proc. Fatigue '81, SEE Fatigue Group Conf.*, Warwick Univ., England (edited by F. Sherratt and J. B. Sturgeon), pp. 97–105. Westbury House, Guildford, England (1981).
41. D. F. Socie, J. D. Morrow and W. C. Chen, *Engng Fract. Mech.* **11,** 851 (1979).
42. D. C. Stouffer and J. F. Williams, *Engng Fract. Mech.* **11,** 525 (1979).
43. G. Glinka, *Int. J. Fatigue* **4,** 59 (1982).
44. M. Kikukawa, M. Jono and Y. Murata, *Proc. Fatigue '81, SEE Fatigue Group Conf.* Warwick Univ. England (edited by F. Sharratt and J. B. Sturgeon), pp. 308–317. Westbury House, Guildford, England (1981).
45. R. J. Donahue, H. Mc I. Clark, P. Atanmo, R. Kumble and A. J. McEvily, *Int. J. Fract. Mech.* **8,** 209 (1972).
46. G. G. Garrett and J. F. Knott, *Metall. Trans. A* **7A,** 884 (1976).
47. B. Tomkins, *Metal Sci.* **14,** 408 (1980).
48. J. F. Knott and A. C. Pickard, *Metal Sci.* **11,** 399 (1977).
49. I. F. C. Smith, Ph.D thesis, Cambr. Univ. Engng Dept. (1982).
50. J. D. Morrow and G. M. Sinclair, *ASTM STP* **237,** 83 (1958).
51. A. Saxena and S. J. Hudak Jr, *ASTM STP* **677,** 215 (1979).
52. B. I. Sandor, *Fundamantals of Cyclic Stress and Strain*, Univ. of Wisconsin Press, Maddison, WI (1972).
53. O. E. Wheeler, *J. Basic Engng, Trans. Am. Soc. Mech. Engrs* **94,** 181 (1972).
54. J. D. Willenborg, R. M. Engle and H. A. Wood, *AFFDL-TM-FBR*-71-1 (1971).

APPENDIX I

The Willenborg et al. *model*

The Willenborg *et al.* retardation model [A1] is based on the assumption that overloads induce compressive residual stresses ahead of the crack tip and thereby reduce crack tip stress intensities by an amount, K_{red}. The quantity K_{red} is a function of the forward plastic zone size associated with the current load cycle of a load sequence and of the overload plastic zone size due to the most severe previous overload. The model predicts crack growth retardation when the nominal minimum stress intensity of the current load cycle is less than K_{red}. In the case of the periodic underloads and periodic overloads considered in this study, K_{min} is always greater than K_{red} and so no retardation is predicted.

The Wheeler model

Wheeler's retardation model [A2] is also based on the supposition that compressive residual stresses ahead of the crack tip lead to retarded growth. It assumes that the crack growth rate due to the current load cycle, ΔK, of a load sequence is equal to the constant amplitude growth rate corresponding to ΔK, multiplied by a retardation factor, ϕ. Wheeler defines ϕ as

$$\phi = \left(\frac{r_p}{d}\right)^m \tag{A1}$$

where r_p is the forward plastic zone size associated with the current load cycle, d is the distance from the crack tip to the overload plastic zone boundary due to the most severe previous overload and m is an adjustable parameter termed the Wheeler index.

References

A1. J. D. Willenborg, R. M. Engle and H. A. Wood, *AFFDL-TM-FBR*-71-1 (1971).
A2. O. E. Wheeler, *J. Basic Engng, Trans. Am. Soc. Mech. Engrs* **94,** 181 (1972).